High-Order Locally Corrected Nyström Solution with Mixed-Order Basis Functions for Electromagnetic Scattering

Stephen D. Gedney, Aiming Zhu & Caicheng Lu
Department of Electrical and Computer Engineering
University of Kentucky
Lexington, KY 40506-0046
gedney@engr.uky.edu

Abstract: A high-order locally-corrected Nyström (LCN) solution of a hybrid volume/surface integral equation is presented for the electromagnetic scattering by complex targets that consist of composite homogeneous and inhomogeneous materials and conducting objects. It is found that for general scattering objects, the use of mixed-order basis functions accelerates the convergence of the LCN solution, eliminates spurious charges, and significantly reduce the condition number of the resulting linear system of equations. Fast iterative solvers based on a multi-level fast multipole method (MLFMM) and the quadrature sampled pre-corrected FFT (QSPCFFT) are also employed to enable the practical solution of large complex targets.

Keywords: Electromagnetic scattering, integral equation methods, locally corrected Nyström method, fast solution methods.

1. Formulation

Consider the electromagnetic interaction with a material scatterer composed of penetrable and conducting materials as illustrated in Fig. 1. A surface separating volumes V_i and V_j is denoted as $S_{i,j}$. Let $S_{i,j}^+$ denote the surface just inside V_i, and $S_{i,j}^-$ denote the surface just inside V_j. Equivalent current densities are then placed on all surfaces separating each material volume and are defined as:

$$\vec{J}_{i,j}^{+} = \hat{n}_i \times \vec{H}\Big|_{S_{i,j}^+}, \quad \vec{M}_{i,j}^{+} = -\hat{n}_i \times \vec{E}\Big|_{S_{i,j}^+}, \; \vec{J}_{i,j}^{-} = \hat{n}_j \times \vec{H}\Big|_{S_{i,j}^-}, \quad \vec{M}_{i,j}^{-} = -\hat{n}_j \times \vec{E}\Big|_{S_{i,j}^-} \tag{1}$$

where $\hat{n}_i$ and $\hat{n}_j$ are the unit normal directed into V_i and V_j, respectively. Since $\hat{n}_j = -\hat{n}_i$,

$$\vec{J}_{i,j}^{+} = -\vec{J}_{i,j}^{-} = \vec{J}_{i,j}, \quad \vec{M}_{i,j}^{+} = -\vec{M}_{i,j}^{-} = \vec{M}_{i,j}. \tag{2}$$

On the surface of a conductor, only the electric current density is supported. Consequently,

$$\vec{J}_{i,p} = \hat{n}_i \times \vec{H}\Big|_{S_{i,p}^+}. \tag{3}$$

Each material volume is assigned a *background* material profile $(\varepsilon_{ib}, \mu_{ib})$. If $(\varepsilon_i, \mu_i) \neq (\varepsilon_{ib}, \mu_{ib})$, this results in the need of an equivalent volume current density, expressed as:

$$\vec{J}_{Vi}(\vec{r}) = j\omega\varepsilon_{ib}\left(\frac{\varepsilon_i(\vec{r})}{\varepsilon_{ib}} - 1\right)\vec{E}(\vec{r}), \quad \vec{M}_{Vi}(\vec{r}) = j\omega\mu_{ib}\left(\frac{\mu_i(\vec{r})}{\mu_{ib}} - 1\right)\vec{H}(\vec{r}) \tag{4}$$

where $(\varepsilon_{ir}, \mu_{ir})$ are the permittivity and permeability of the physical material medium.

If $(\varepsilon_i, \mu_i) = (\varepsilon_{ib}, \mu_{ib})$, the volume current densities are zero. Also, if $(\varepsilon_{jb}, \mu_{jb}) = (\varepsilon_{ib}, \mu_{ib})$, the

Report Documentation Page

Form Approved
OMB No. 0704-0188

1. REPORT DATE	2. REPORT TYPE	3. DATES COVERED
23 APR 2004	**N/A**	**-**

4. TITLE AND SUBTITLE	5a. CONTRACT NUMBER
High-Order Locally Corrected Nyström Solution with Mixed-Order Basis Functions for Electromagnetic Scattering	5b. GRANT NUMBER
	5c. PROGRAM ELEMENT NUMBER
6. AUTHOR(S)	5d. PROJECT NUMBER
	5e. TASK NUMBER
	5f. WORK UNIT NUMBER
7. PERFORMING ORGANIZATION NAME(S) AND ADDRESS(ES) **Department of Electrical and Computer Engineering University of Kentucky Lexington, KY 40506-0046**	8. PERFORMING ORGANIZATION REPORT NUMBER
9. SPONSORING/MONITORING AGENCY NAME(S) AND ADDRESS(ES)	10. SPONSOR/MONITOR'S ACRONYM(S)
	11. SPONSOR/MONITOR'S REPORT NUMBER(S)

12. DISTRIBUTION/AVAILABILITY STATEMENT
Approved for public release, distribution unlimited

13. SUPPLEMENTARY NOTES
See also ADM001763, Annual Review of Progress in Applied Computational Electromagnetics (20th) Held in Syracuse, NY on 19-23 April 2004., The original document contains color images.

14. ABSTRACT

15. SUBJECT TERMS

16. SECURITY CLASSIFICATION OF:			17. LIMITATION OF ABSTRACT	18. NUMBER OF PAGES	19a. NAME OF RESPONSIBLE PERSON
a. REPORT	b. ABSTRACT	c. THIS PAGE			
unclassified	**unclassified**	**unclassified**	**UU**	**6**	

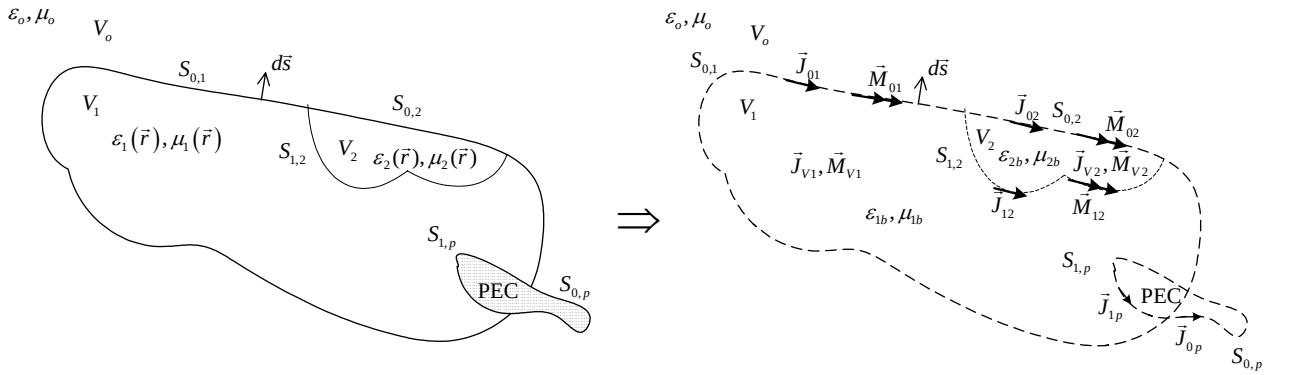

Fig. 1 Equivalent currents representing the scattered fields due to a plane wave impinging on an arbitrary inhomogeneous material scatterer.

surface current densities on $S_{i,j}$ will be zero.

Each equivalent current density radiates in an equivalent homogeneous material volume. For example, $\vec{J}^{+}_{i,j}, \vec{M}^{+}_{i,j}, \vec{J}_{Vi}, \vec{M}_{V_i}$ are effectively radiating in a homogeneous space with material profile $(\varepsilon_{ib}, \mu_{ib})$. Thus, the *scattered* field radiated by the equivalent currents in V_i can be expressed as:

$$\vec{E}_i^{scat}\left(\vec{J}_{eq}, \vec{M}_{eq}\right) = \eta_{ib}\mathbf{L}_i\left(\vec{J}_{eq}\right) - \mathbf{K}_i\left(\vec{M}_{eq}\right) \tag{5}$$

$$\vec{H}_i^{scat}\left(\vec{J}_{eq}, \vec{M}_{eq}\right) = \mathbf{K}_i\left(\vec{J}_{eq}\right) + \eta_{ib}^{-1}\mathbf{L}_i\left(\vec{M}_{eq}\right) \tag{6}$$

where,

$$\mathbf{L}_i\left(\vec{X}_{eq}\right) = -jk_{ib}\int_{\Omega}\left[\bar{\bar{I}} + \frac{1}{k_{ib}^2}\nabla\nabla\right]\cdot\vec{X}_{eq}\left(\vec{r}'\right)G_i\left(\vec{r},\vec{r}'\right)d\Omega' \tag{7}$$

$$\mathbf{K}_i\left(\vec{X}_{eq}\right) = \int_{\Omega}\nabla\times G_i\left(\vec{r},\vec{r}'\right)\vec{X}_{eq}\left(\vec{r}'\right)d\Omega' \tag{8}$$

where Ω is either a surface or volume, $\bar{\bar{I}}$ is the idem factor, or unit diad, $G_i\left(\vec{r},\vec{r}'\right) = e^{-jk_{ib}|\vec{r}-\vec{r}'|}/4\pi|\vec{r}-\vec{r}'|$, $k_{ib} = \omega\sqrt{\varepsilon_{ib}\mu_{ib}}$ and $\eta_{ib} = \sqrt{\mu_{ib}/\varepsilon_{ib}}$.

The proposed method of moment solution is based on a hybrid surface/volume integral formulation with the appropriate constraints applied on boundary surfaces and within material volumes. At a surface $S_{i,j}$ separating two material regions, the surface integral formulation is derived via a combined field formulation based on Müller's formulation, leading to [1, 2]:

$$\vec{t}_s\cdot\varepsilon_{r_i}\vec{E}_i^{inc}\Big|_{S_{i,j}^{+}} + \vec{t}_s\cdot\varepsilon_{r_j}\vec{E}_j^{inc}\Big|_{S_{i,j}^{-}} = \vec{t}_s\cdot\hat{n}_i\times\vec{M}_{i,j}\left(\varepsilon_{r_i}+\varepsilon_{r_j}\right) - \vec{t}_s\cdot\varepsilon_{r_i}\vec{E}_i^{scat}\Big|_{S_{i,j}^{+}} - \vec{t}_s\cdot\varepsilon_{r_j}\vec{E}_j^{scat}\Big|_{S_{i,j}^{-}} \tag{9}$$

$$\vec{t}_s\cdot\mu_{r_i}\vec{H}^{inc}\Big|_{S_{i,j}^{+}} + \vec{t}_s\cdot\mu_{r_j}\vec{H}^{inc}\Big|_{S_{i,j}^{-}} = -\vec{t}_s\cdot\hat{n}_i\times\vec{J}_{i,j}\left(\mu_{r_i}+\mu_{r_j}\right) - \vec{t}_s\cdot\mu_{r_i}\vec{H}^{scat}\Big|_{S_{i,j}^{+}} - \vec{t}_s\cdot\mu_{r_j}\vec{H}^{scat}\Big|_{S_{i,j}^{-}} \tag{10}$$

where $\vec{E}_i^{inc}, \vec{H}_i^{inc}$ are radiated by impressed sources in V_i, $\vec{E}_i^{scat}, \vec{H}_i^{scat}$ are radiated by equivalent currents in volume V_i (similarly for subscript *j*), $\hat{n}_i$ is the unit normal to $S_{i,j}$ and directed into V_i, and $\vec{t}_s$ is a test vector tangential to $S_{i,j}$. Müller's formulation has the advantage over the classical PMCHWT (Poggio, Miller, Chang, Harrington, Wu and Tai) formulation [3] in that it behaves as a second-kind integral equation for moderate to low contrast materials. Furthermore, the hyper-singularity of the $\mathbf{L}$-operator in is reduced by one order and we have found it leads a reduction in the condition number of the matrix arising from the LCN method.

On the surface of a conductor, a combined field integral operator (CFIE) is applied [4]:

$$\frac{\alpha}{\eta_{ib}}\hat{t}_p \cdot \vec{E}_i^{inc}\Big|_{S_{i,p}} + (1-\alpha)\hat{t}_p \cdot \hat{n} \times \vec{H}_i^{inc}\Big|_{S_{i,p}} = \frac{\alpha}{\eta_{ib}}\left(Z_s \hat{t}_p \cdot \vec{J}_{i,p} - \hat{t} \cdot \vec{E}_i^{scat}\Big|_{S_{i,p}} \right) + (1-\alpha)\left(\hat{t}_p \cdot \vec{J}_{i,p} - \hat{t}_p \cdot \hat{n} \times \vec{H}_i^{scat}\Big|_{S_{i,p}} \right) \tag{11}$$

where Z_s is the Leonotovich surface impedance, and $\hat{t}_p$ is a test vector tangential to the conductor surface $S_{i,p}$. Finally, in regions where the volume currents are non-zero, the constraints applied are:

$$\vec{E}_i^{inc}(\vec{r}) = \vec{J}_{V_i}(\vec{r}) \Big/ \left(j\omega\varepsilon_{ib}\left(\varepsilon_i(\vec{r})/\varepsilon_{ib} - 1\right)\right) - \vec{E}_i^{scat}(\vec{r}) \tag{12}$$

$$\vec{H}_i^{inc}(\vec{r}) = \vec{M}_{V_i}(\vec{r}) \Big/ \left(j\omega\mu_{ib}\left(\mu_i(\vec{r})/\mu_{ib} - 1\right)\right) - \vec{H}_i^{scat}(\vec{r}). \tag{13}$$

where $\vec{r} \in V_i$.

2. Discretization

It is assumed that the volume regions (as needed) and surfaces are discretized using curvilinear cells that represent all boundaries and material inhomogeneities to high-order accuracy. In this work, volume cells are assumed to be curvilinear hexahedron and surface cells are assumed to be curvilinear quadrilaterals. The current density is then expanded over each cell using a set of local vector basis functions. To date, LCN formulations have employed current basis functions that are complete to a polynomial order [5, 6]. Here, the vector basis used are mixed-order basis functions, described as [7]:

$$\vec{J}_1^{mo}(u^1,u^2) = \vec{a}_1 P_j(u^1) P_k(u^2)/\sqrt{g} \quad (j = 0..p; k = 0..p-1), \tag{14}$$

$$\vec{J}_2^{mo}(u^1,u^2) = \vec{a}_2 P_j(u^1) P_k(u^2)/\sqrt{g} \quad (j = 0..p-1; k = 0..p), \tag{15}$$

on surface patches, or

$$\vec{J}_1^{mo}(u^1,u^2,u^3) = \vec{a}_1 P_j(u^1) P_k(u^2) P_l(u^3)/\sqrt{g} \quad (j = 0..p; k,l = 0..p-1), \tag{16}$$

$$\vec{J}_2^{mo}(u^1,u^2,u^3) = \vec{a}_2 P_j(u^1) P_k(u^2) P_l(u^3)/\sqrt{g} \quad (k = 0..p; j,l = 0..p-1), \tag{17}$$

$$\vec{J}_3^{mo}(u^1,u^2,u^3) = \vec{a}_3 P_j(u^1) P_k(u^2) P_l(u^3)/\sqrt{g} \quad (j,k = 0..p-1;\ l = 0..p) \tag{18}$$

over a volume cell. Note that the same basis functions are used for magnetic current densities. For this choice of basis functions, the charge density (derived from the divergence of the surface current density) is effectively described by a polynomial expansion, complete to order *p*. It was shown in [7] by Çalişkan and Peterson and further demonstrated by Gedney, Zhu, and Lu in [8] that polynomial complete current basis can lead to spurious solutions for problems with edge singularities and that this can be remedied through the use of the mixed-order basis. This is somewhat intuitive for the following reason. If one observes the charge density at the edge singularity, one expects the charge density to exhibit the same leading-order singularity as the current flowing transverse to the edge and as the normal derivative of the current flowing normal to the edge. This can be well approximated by the mixed-order basis. For the polynomial complete basis this is approximated by the lower-order terms, but there are additional spurious charge terms from the highest-order basis that exist. For smooth scatterers, this does not occur and consequently either basis function can be used successfully. However, it appears that since the charge density is over-specified by the polynomial-complete basis, a poorly conditioned system results for the EFIE or CFIE operators.

When employing the mixed-order basis functions, an appropriate testing scheme must be implemented within the context of the LCN method. This is done by introducing an appropriate quadrature rule over each cell. For a surface curvilinear quadrilateral cell, the quadrature rules are represented by the product of two one-dimensional Guass-quadrature rules. For a volume curvilinear hexahedron, the product of three one-dimensional Gauss-quadrature rules are used. For a surface cell, two different quadrature rules are used: a $(p+1)\times p$ -point rule and a $p\times(p+1)$ -point rule. Three-quadrature rules are introduced for the volume cells.

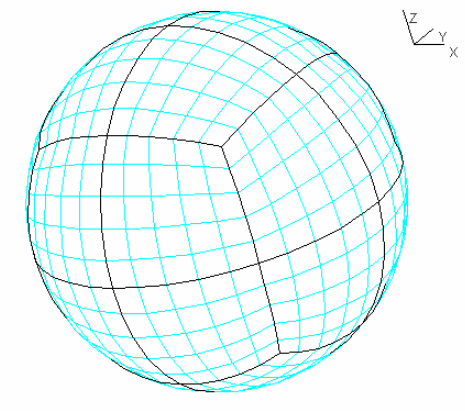

Fig. 2. Curvilinear quadrilateral cell discretization of a spherical surface (24, 5th-order cells).

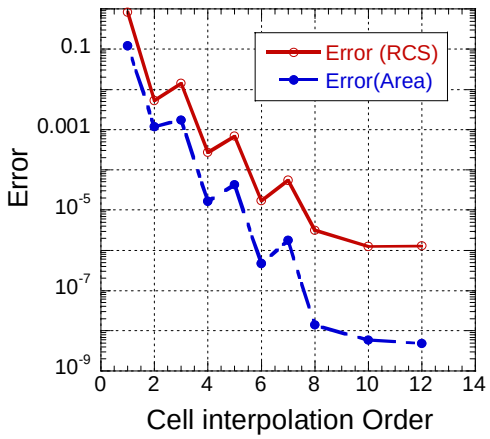

Fig. 3 Relative mean error in the RCS computed via the LCN method with ninth-order basis and area of a sphere of radius $k_o a = 6$ versus the interpolation order of the 24 curvilinear cells.

For each rule, a test vector $\vec{t}_i$ is introduced. The vector dot product of the appropriate integral operator is taken with the test vector $\vec{t}_i$ at the abscissa points of the quadrature rule. This collocation scheme leads to a linear system of equation. It is noted that the choice of the test vectors is quite important. Best results are obtained if the test vectors diagonalize the constant terms of the integral operators. Thus, for the surface integral operators in (9) – (11) suitable test vectors are:

$$\vec{t}_{s_1} = -\vec{a}_2,\ \vec{t}_{s_2} = \vec{a}_1,\ \vec{t}_{p_i} = \vec{a}^{\,i},\ (i = 1,2), \tag{19}$$

where $\vec{a}^{\,i}$ is the reciprocal unitary vector [9]. Test vectors applied to the volume integral equations in (12) and (13) are:

$$\vec{t}_{V_i} = \vec{a}^{\,i},\ (i = 1,3). \tag{20}$$

3. Numerical Results

The above formulation has been incorporated into a single program. The software is capable of analyzing general composite material scatterers composed of inhomogeneous or piecewise homogeneous dielectric, magnetic and conducting materials with an arbitrary number of regions. The surfaces and volumes are discretized with curvilinear quadrilateral and hexahedral elements. The use of high-order curvilinear cells is critical for the efficient implementation of a high-order solution scheme. The reason for this is that a high-order scheme is typically most efficient when applied to electrically large cells with high-order basis functions. The reason for this is that the higher the order of the basis, the steeper the slope of the error curve. However, the patches must also accurately represent the surfaces they are modeling. Else, the result can suffer from discretization error. Consequently, curvilinear cells must be employed. To demonstrate this, consider the electromagnetic scattering by a PEC sphere of radius *a* defined by $k_o a = 6$. The sphere was discretized with 24 quadrilateral curvilinear cells as illustrated in Fig. 2. Initially, the *basis function order* was set to *p* = 9. 10×9 and 9×10-point Gauss-Legendre quadrature rules were used for the Nyström discretization of each patch. Then, the order of the *cells* was increased from *n* = 1 to *n* = 12. The bistatic RCS was then computed for the sphere and the mean relative error was calculated relative to a Mie-series solution as:

$$\text{Mean Error} = \frac{1}{N_a} \sum_{i=1}^{N_a} \frac{\left| \sigma^{LCN}(\theta_i, \phi_i) - \sigma^{Mie}(\theta_i, \phi_i) \right|}{\left| \sigma^{Mie}(\theta_i, \phi_i) \right|} \tag{21}$$

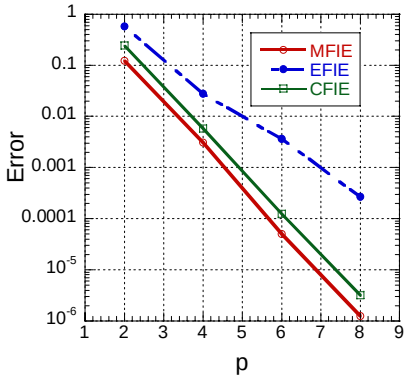

Fig. 4 Relative mean error of RCS for a sphere of radius $k_o a = 6$ versus the basis order *p*.

where N_a is the number of angles (360 uniformly spaced angles were computed). A graph of the mean relative error versus the cell order *n* computed for the MFIE is illustrated in Fig. 3. The error in the area of the sphere as approximated via the Gauss-Legendre quadrature rule is also graphed in Fig. 2 as a comparison. Initially, it is observed that error in the RCS and the area follow the same general trend. It also appears that the minimum error is reached when $n = p+1$. This emphasizes the need for isoperimetric curvilinear cells to accurately represent the surface to realize the full potential of the high-order solution scheme. The error in the RCS was also computed as a function of basis order. In each case, the cell order *n* is set so that *n* = *p*+1. The RCS was predicted via the MFIE ($\alpha = 0$ in (11)), the EFIE ($\alpha = 1$) and the CFIE ($\alpha = 0.1$), and the mean error was predicted via (21). A graph of the mean relative error versus order *p* is illustrated in Fig. 4 for *p* = 2, 4, 6, and 8.

Next, consider the EMCC double metallic ogive [10]. A 288 cell discretization of the ogive is illustrated in Fig. 5. The ogive is 7.5 in long, and has a maximum radius of 1 in. The monstatic RCS of the ogive at 9 GHz is illustrated in Fig. 6. This compares extremely well to the measured and calculated data in [10].

Finally, consider the coated double ogive in Fig. 7. The ogive is coated with a thin dielectric coating with a homogeneous dielectric of relative permittivity $\varepsilon_r = 9 - j0.3$. The coating has a length of 8.25 in, and a maximum radius of 1.1 in. The RCS of the coated ogive at 1.57 GHz is illustrated in Fig. 8. Different orders are illustrated to demonstrate that the results have converged.

References

[1] C. Müller, *Foundations of the Mathematical Theory of Electromagnetic Waves*, vol. 301. Berlin: Springer-Verlag, 1969.

[2] R. F. Harrington, "Boundary integral formulations for homogeneous material bodies," *Journal of Electromagnetic Waves and Applications*, vol. 3, pp. 1-15, 1989.

[3] X. Q. Sheng, J. M. Jin, J. M. Song, W. C. Chew, and C. C. Lu, "Solution of combined-field integral equation using multilevel fast multipole algorithm for scattering by homogeneous bodies," *IEEE Transactions on Antennas and Propagation*, vol. 46, pp. 1718-1726, 1998.

[4] A. F. Peterson, S. L. Ray, and R. Mittra, *Computational Methods for Electromagnetics*. New York: IEEE Press, 1998.

[5] L. F. Canino, J. J. Ottusch, M. A. Stalzer, J. L. Visher, and S. M. Wandzura, "Numerical solution of the Helmholtz equation in 2D and 3D using a high-order Nyström discretization," *Journal of Computational Physics*, vol. 146, pp. 627-663, 1998.

[6] S. D. Gedney, "On Deriving a Locally Corrected Nyström Scheme from a Quadrature Sampled Moment Method," *IEEE Transactions on Antennas and Propagation*, vol. 51, pp. 2402-2412, 2003.

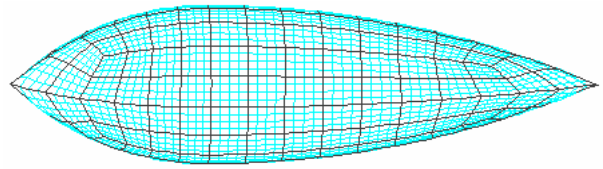

Fig. 5 Curvilinear cell discretization of the EMCC double ogive.

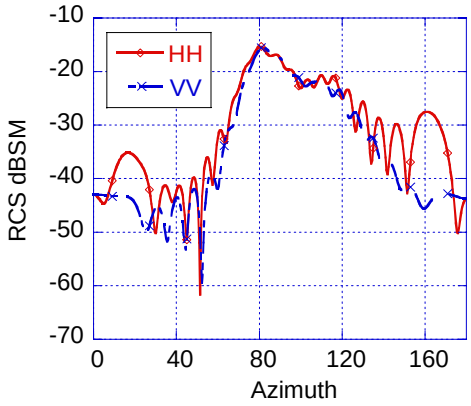

Fig. 6 Monstatic RCS of the conducting double ogive at 9 GHz.

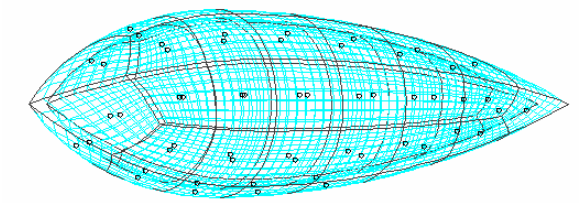

Fig. 7 EMCC double ogive with a thin dielectric coating.

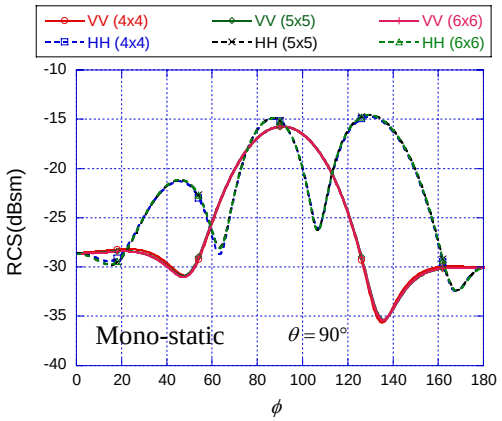

Fig. 8 Monstatic RCS of the coated EMCC dielectric ogive.

[7] F. Çaliskan and A. F. Peterson, "The need for mixed-order representations with the locally corrected Nystrom method," *IEEE Antennas and Wireless Propagation Letters*, vol. 2, pp. 72- 73, 2003.

[8] S. D. Gedney, A. Zhu, and C. C. Lu, "Study of mixed-order basis functions for the locally-corrected Nyström method," *IEEE Transactions on Antennas and Propagation*, submitted, October 2003.

[9] J. A. Stratton, *Electromagnetic Theory*. New York: McGraw-Hill, 1941.

[10] A. C. Woo, H. T. G. Wang, and M. J. Schuh, "Benchmark radar targets for the validation of computational electromagnetics programs," *IEEE Antennas and Propagation Magazine*, vol. 35, pp. 84-89, 1993.

